Fully Analytic Compact Model of Ballistic Gate-All-Around MOSFET with Rectangular Cross Section

Tatsuhiro Numata[1,4], Shigeyasu Uno[2,4], Yoshinari Kamakura[3,4], Nobuya Mori[3,4], and Kazuo Nakazato[1]
[1]Department of Electrical and Computer Science, Graduate School of Engineering, Nagoya University
Furo-cho, Chikusa-ku, Nagoya 464-8603, Japan
Phone: +81-52-789-2794, Fax: +81-52-789-3139,
E-mail: t_numata@echo.nuee.nagoya-u.ac.jp, suno@fc.ritsumei.ac.jp
[2]Department of Photonics, College of Science and Engineering, Ritsumeikan University
1-1-1 Noji-Higashi, Kusatsu, Shiga, 525-8577, Japan
[3]Department of Electronic Engineering, Osaka University 2-1 Yamada-oka, Suita, Osaka 565-0871, Japan
[4]JST, CREST, 5 Sanbancho, Chiyoda-ku, Tokyo 102-0075, Japan

***Abstract*—We develop a fully analytic compact model of gate-all-around metal-oxide-semiconductor field-effect transistors in the ballistic transport. The potential shape in the wire cross section is approximated by a parabolic function. With the model potential, electron energy levels are derived analytically and have an unknown parameter. The electron energy levels are determined by solving approximately the coupled equation of charge densities derived from quantum mechanics and electrostatics. We solve the coupled equation with the Aymerich approximation technique. The unknown parameter and also electron energy levels can be derived analytically. Device characteristics calculated from the analytic model are compared with the model with the unknown parameter obtained numerically, demonstrating an excellent accuracy. We carry out a circuit simulation with the analytic model of ballistic gate-all-around metal-oxide-semiconductor field-effect transistors.**

***Index Terms*—GAA-MOSFETs, ballistic transport, analytic model, perturbation theory, circuit simulation**

I. Introduction

Gate-all-around (GAA) metal-oxide-semiconductor field-effect transistors (MOSFETs) have been studied extensively owing to their excellent controllability of the electrostatic potential in the channel and attracted considerable attention as a next-generation semiconductor device. Several computational techniques of electron states based on the quantum transport such as non-equilibrium Green's function (NEGF) formalism have been proposed [1], [2], with which the ballistic current of GAA-MOSFETs is evaluated numerically. However, it is not practical to introduce such numerical methods into the circuit simulator such as SPICE due to an immense amount of simulation time. Some compact models of ballistic GAA-MOSFETs have been already reported [3]–[5], but these models rely on coupled equations to be evaluated numerically. Although an analytic circuit model without numerical calculation is proposed [6], the model contains parameters that have to be determined numerically in advance. Thus, a fully analytic and explicit compact model has not yet proposed.

In this work, we propose a fully analytic compact model for ballistic GAA-MOSFETs with a rectangular wire cross section, and we demonstrate a circuit simulation using the model.

II. Ballistic Current

We consider GAA-MOSFETs of gate length $L_{\rm G}$, channel width t_x, channel height t_y and gate oxide thickness $t_{\rm ox}$ with a rectangular cross section, as shown in Fig. 1. Figure 2(a) shows the schematic potential profile along the electron transport direction. Ballistic current is determined by electrons that have energy level larger than $E_{\rm max}$ in the source or drain electrode. Then, ballistic current is given by [3]:

$$I_{\rm DS} = \frac{ek_{\rm B}T}{\pi\hbar} \times \sum_{n_v}\sum_{n} \ln\left\{\frac{1+\exp\left[\left(E_{\rm FS}-E_{n_v,n}\right)/k_{\rm B}T\right]}{1+\exp\left[\left(E_{\rm FD}-E_{n_v,n}\right)/k_{\rm B}T\right]}\right\}, \quad (1)$$

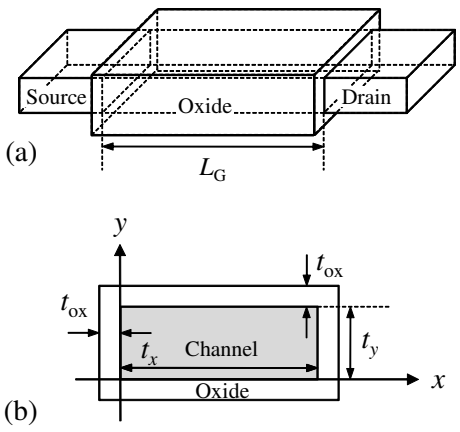

Fig. 1. Structure of a GAA-MOSFET. (a) Schematic view of a GAA-MOSFET that has the rectangular wire channel with gate length $L_{\rm G}$. (b) Wire cross section of channel width t_x, channel height t_y and oxide thickness $t_{\rm ox}$.

978-1-61284-418-3/11/$26.00 © 2011 IEEE

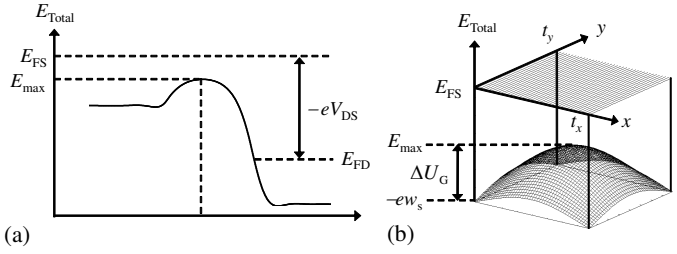

Fig. 2. Schematic potential energy distribution in the GAA-MOSFET. (a) Potential profile along the electron transport direction, where $E_{\max}$ is the top of the barrier in the channel. Fermi levels at the source and drain are denoted as E_{FS} and $E_{\text{FD}}(= E_{\text{FS}} - eV_{\text{DS}})$. (b) Potential profile in the wire cross section at the barrier top.

where n is quantum number in the wire cross section, and $E_{n_v,n}$ represents a confinement energy level at the barrier top, belonging to the specific valley n_v for the channel material. Ballistic current depends only on energy levels at the barrier top as shown (1). If an analytic expression of $E_{n_v,n}$ is obtained, the fully analytic model of ballistic current is derived.

III. Numerical Compact Model

Figure 2(b) shows the schematic potential profile in the wire cross section at the barrier top. Firstly, the potential shape in the wire cross section is approximated by a parabolic function as a model potential:

$$w(x,y) = w_{\text{s}}(\Delta U_{\text{G}}) - 4\Delta U_{\text{G}} f(x,y), \tag{2}$$

$$f(x,y) = \frac{x}{t_x+t_y}\left(1-\frac{x}{t_x}\right) + \frac{y}{t_x+t_y}\left(1-\frac{y}{t_y}\right), \tag{3}$$

where ΔU_{G} determines the potential shape in the wire cross section in Fig. 2(b), and $w_{\text{s}}(\Delta U_{\text{G}})$ represents electrostatic potential at the interface between the oxide and the channel. Electron states in the wire cross section are derived by solving the Schrödinger equation. With the model potential, the Schrödinger equation can be separated into x- and y-direction. The Schrödinger equation along x-axis is then written by:

$$\left[-\frac{\hbar^2}{2m_x^*}\frac{d^2}{dx^2} + 4e\Delta U_{\text{G}} f(x,0)\right]\psi_{n_v,n_x}(x) = E^{\text{q}}_{n_v,n_x}\psi_{n_v,n_x}(x), \tag{4}$$

where m_x^* is electron effective mass, ψ_{n_v,n_x} represents the wave functions of electrons, and $E^{\text{q}}_{n_v,n_x}$ is a confinement energy level. The energy level with the superscript q is measured from $-ew_{\text{s}}$. Equation (4) can be solved approximately with the perturbation theory, and, as a result, the electron energy levels are obtained as a quadratic function of ΔU_{G} by considering the second-order term of the perturbation as follows:

$$E^{\text{q}}_{n_v,n_x}(\Delta U_{\text{G}}) = E^{\text{q0}}_{n_v,n_x} + (e\Delta U_{\text{G}})H_{n_x,n_x} + (e\Delta U_{\text{G}})^2 \sum_{n'_x \neq n_x} \frac{\left|H_{n'_x,n_x}\right|^2}{E^{\text{q0}}_{n_x} - E^{\text{q0}}_{n'_x}}, \tag{5}$$

where $H_{n'_x,n_x}$ represents a matrix element [7], which is obtained analytically. In the summation in (5), we consider a sufficient number of n'_x. When $n'_x = n_x$,

$$H_{n'_x,n_x} = \frac{t_x}{t_x+t_y}\left[\frac{2}{3} + \frac{2}{(1+n'_x)^2\pi^2}\right], \tag{6}$$

and when $n'_x \neq n_x$,

$$H_{n'_x,n_x} = -16\frac{t_x(n_x+1)(n'_x+1)}{(t_x+t_y)\pi^2} \times \left[\frac{1+(-1)^{n_x+n'_x+2}}{(n_x-n'_x)^2(n_x+n'_x+2)}\right]. \tag{7}$$

Electron energy levels E_{n_v,n_x,n_y} measured from E_{FS} are given by:

$$E_{n_v,n_x,n_y}(\Delta U_{\text{G}}) = E^{\text{q}}_{n_v,n_x}(\Delta U_{\text{G}}) + E^{\text{q}}_{n_v,n_y}(\Delta U_{\text{G}}) - ew_{\text{s}}(\Delta U_{\text{G}}), \tag{8}$$

where $E^{\text{q}}_{n_v,n_y}$ can be derived in the similar procedure mentioned above. With (1), (5) and (8), ballistic current is derived as a function of ΔU_{G}. The quantity ΔU_{G} is determined by solving the coupled equation of the charge densities derived from the quantum mechanics, Q_{q}, and electrostatics, Q_{e}, under each bias condition [7]. The charge density, Q_{q}, is given by:

$$Q_{\text{q}}(\Delta U_{\text{G}}) = -e\frac{\sqrt{2m_z^* k_{\text{B}}T}}{\pi\hbar}\sum_{n_v}\sum_{n_x}\sum_{n_y} \times \left[F_{-\frac{1}{2}}\left(\frac{-E_{n_v,n_x,n_y}(\Delta U_{\text{G}})}{k_{\text{B}}T}\right) + F_{-\frac{1}{2}}\left(\frac{-eV_{\text{DS}} - E_{n_v,n_x,n_y}(\Delta U_{\text{G}})}{k_{\text{B}}T}\right)\right], \tag{9}$$

where $F_{-1/2}(u)$ represents Fermi-integral referred in [5]. On the other hand, the charge density, Q_{e}, is derived from the Poisson equation and the model potential:

$$Q_{\text{e}}(\Delta U_{\text{G}}) = -8\varepsilon_{\text{ch}}\Delta U_{\text{G}}, \tag{10}$$

where ε_{ch} is a permittivity associated with the channel material. The coupled equation $Q_{\text{q}} = Q_{\text{e}}$ requires a surface potential w_{s} through (8). The surface potential is derived from the boundary condition at the interface between oxide and the channel as follows:

$$\frac{t_x+t_y}{2}V'_{\text{GS}} = \int_0^{t_x/2} dx\,[w(x,0) + V_{\text{ox}}(x)] + \int_0^{t_y/2} dy\,[w(0,y) + V_{\text{ox}}(y)], \tag{11}$$

$$V'_{\text{GS}} = V_{\text{GS}} - \phi_{\text{GC}} + w_{\text{FB}}, \tag{12}$$

where ϕ_{GC} is difference of the workfunction between gate and channel materials, and w_{FB} represents the conduction band edge measured from $E_{\text{FS}}/(-e)$ at the flat-band condition, which is determined by workfunction and electron affinity of the channel material. The voltage drop across the gate oxide V_{ox} is derived, which satisfies the continuity of the electric displacement at the interface between the oxide and channel.

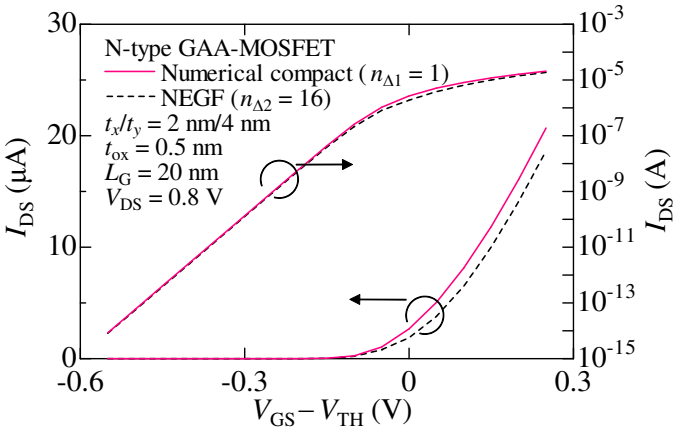

Fig. 3. Ballistic current characteristics calculated from numerical compact model (solid line) and NEGF simulation (dashed line) as a function of V_{GS}. We define V_{TH} as the gate voltage at which the lowest energy level reaches E_{FS}. A parameter $n_{\Delta 1}$ represents the number of energy levels considered in (1) and (9) for the numerical compact model, and $n_{\Delta 2}$ represents the number of energy levels considered in the NEGF simulation.

From (11), the surface potential w_s is derived as a function of ΔU_G as follows:

$$w_s(\Delta U_G) = V'_{GS} + \Delta U_G \widetilde{V}_{ox}, \tag{13}$$

$$\widetilde{V}_{ox} = \frac{2}{3}\frac{t_x^2 + t_y^2}{(t_x + t_y)^2} - 4\frac{\varepsilon_{ch} t_{ox}}{\varepsilon_{ox}(t_x + t_y)}, \tag{14}$$

where ε_{ox} is a permittivity associated with the oxide material. The coupled equation with (13) cannot be solved explicitly, so ΔU_G must be determined by either approximately or numerically. The ballistic current is described by the Landauer formula [3] with the obtained energy levels (8) as a function of ΔU_G, and the ballistic current can be evaluated with the obtained ΔU_G. In this calculation, we assumed that the channel and oxide materials are intrinsic Si and SiO_2, respectively, and the transverse and longitudinal effective masses are fixed at $m_t = 0.19m_0$ and $m_l = 0.91m_0$ in a (100)-oriented Si channel. Figure 3 shows a comparison of the ballistic current calculated from the compact model with ΔU_G determined numerically with NEGF simulator [2], demonstrating a reasonable accuracy.

IV. Analytic and Explicit Compact Model

Characteristics of GAA-MOSFETs can be calculated without any numerical calculation if gate and drain voltage dependence of ΔU_G is obtained analytically. We take two assumptions to solve the coupled equation mentioned above

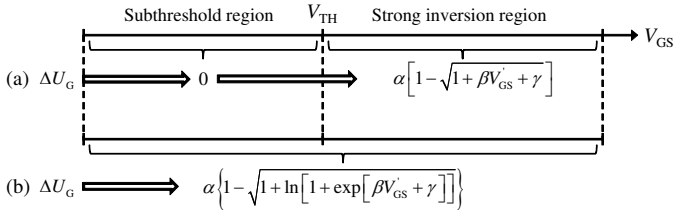

Fig. 4. Analytic expressions of ΔU_G. Parameters α, β and γ are determined from structural parameters. (a) Expressions of ΔU_G in the subthreshold and the strong inversion region. (b) An unified expression of ΔU_G.

to derive an analytic expression of ΔU_G. Firstly, electrons that occupy the lowest energy level are dominant for ballistic current. Secondly, the drain voltage V_{DS} is sufficiently large, that is, $eV_{DS} \gg k_B T$, and the second term in (9) can be ignored. In the subthreshold region, electron density in the wire cross section is sufficiently small. Potential profile in the wire cross section becomes almost the flat-band. Thus, ΔU_G is approximated from (10) as follows:

$$\Delta U_G \approx 0. \tag{15}$$

On the other hand, in the strong inversion region, Q_q is described by the Fermi-integral which is dealt analytically by an approximation technique [8]. With the approximation method, the Fermi-integral in the strong inversion region is written by a polynominal function.

$$F_n(u) = \frac{u^{n+1}}{n+1}, \qquad u \gg 1 \tag{16}$$

With this approximation, the coupled equation $Q_q = Q_e$ in the inversion region is rewritten as:

$$-8\varepsilon_{ch}\Delta U_G = -e\frac{\sqrt{2m_z^* k_B T}}{\pi\hbar} g_v \times \left[\frac{-e(V'_{GS} - \Delta U_G \widetilde{V}_{ox}) - E^q_{1,0,0}(\Delta U_G)}{k_B T}\right]^{\frac{1}{2}}, \tag{17}$$

where g_v represents the valley degeneracy for the lowest energy level. We can solve (17) analytically for ΔU_G,

$$\Delta U_G = \frac{-b_R}{2(a_L + a_R)} \times \left\{1 - \sqrt{1 + \frac{4\left(-eV'_{GS}/k_B T + c_R\right)(a_L + a_R)}{b_R^2}}\right\}, \tag{18}$$

where parameters a_L, a_R, b_R, and c_R are shown in Table. I. Finally, two asymptotic expressions (15) and (18) are connected smoothly as shown in Fig. 4(a) and 4(b). Thus, a fully

TABLE I
Parameters used in (18).

$a_L = \left\{\frac{8\varepsilon_{ch}\pi\hbar}{e g_v}\right\}^2 \frac{1}{2m_z^* k_B T}$,	$a_R = \frac{e^2}{k_B T}\left(\sum_{n'_x \neq n_x} \frac{\lvert H_{0,n'_x}\rvert^2}{E^{q0}_{1,0_x} - E^{q0}_{1,n'_x}} + \sum_{n'_y \neq n_y} \frac{\lvert H_{0,n'_y}\rvert^2}{E^{q0}_{1,0_y} - E^{q0}_{1,n'_y}}\right)$
$b_R = \frac{-e}{k_B T}(H_{0,0} - \widetilde{V}_{ox})$,	$c_R = -\frac{E^{q0}_{1,0_x} + E^{q0}_{1,0_y}}{k_B T}$

$$\Delta U_{\rm G} = \frac{-b_{\rm R}}{2(a_{\rm L}+a_{\rm R})}\left\{1-\sqrt{1+\ln\left[1+\exp\left[\frac{4(-eV'_{\rm GS}/k_{\rm B}T+c_{\rm R})(a_{\rm L}+a_{\rm R})}{b_{\rm R}^2}\right]\right]}\right\}. \quad (19)$$

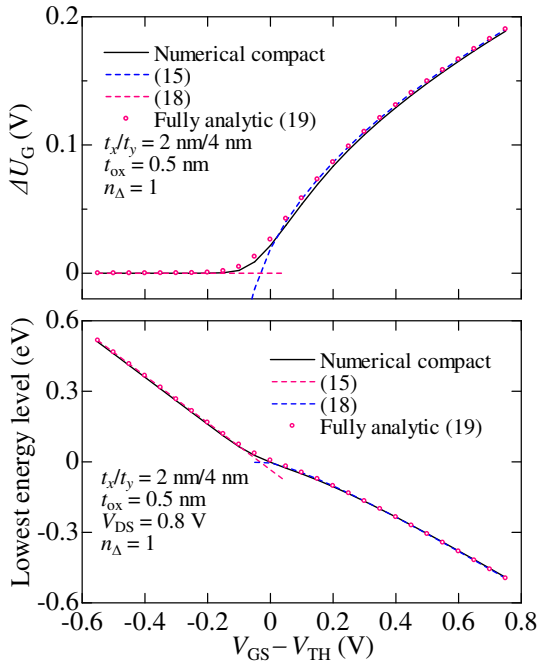

Fig. 5. (a) A parameter $\Delta U_{\rm G}$ calculated from numerical compact model (solid line) and fully analytic model (open circle) as a function of $V_{\rm GS}$. (b) The lowest energy levels calculated from numerical compact model (solid line) and fully analytic model (open circle) as a function of $V_{\rm GS}$, measured from $E_{\rm FS}$, and $n_{\rm s}$ represents the number of energy levels considered in (1) for the fully analytic model.

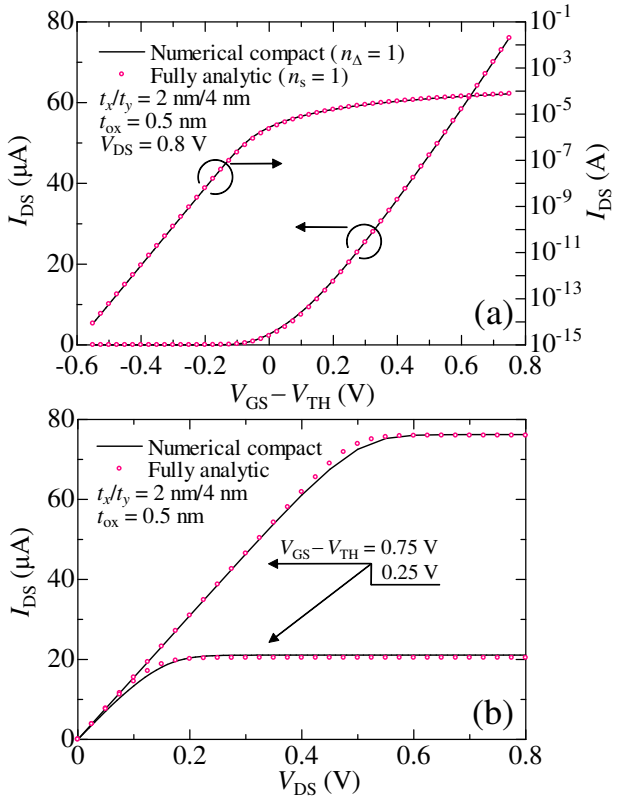

Fig. 6. Current characteristics calculated from numerical compact model (solid line) and fully analytic model (open circle). (a) Gate voltage dependence of the ballistic current for $V_{\rm DS} = 0.8$ V. (b) Drain voltage dependence of the ballistic current for $V_{\rm GS} - V_{\rm TH} = 0.75$ V and 0.25 V.

analytic expression of $\Delta U_{\rm G}$ is obtained, which depends only on structural and bias parameters in (19). The ballistic current depends only on the electron energy levels which is derived in terms of $\Delta U_{\rm G}$. Therefore, a fully analytic and explicit compact model of the drain current for ballistic GAA-MOSFETs is obtained. Figure 5(a) shows the comparison of $\Delta U_{\rm G}$ as a function of $V_{\rm GS}$ with (15), (18), (19) and the compact model with the numerically derived $\Delta U_{\rm G}$ referred in the previous section. As shown in Fig. 5(a), the fully analytic model (19) approach 0 in the subthreshold region and (18) in the strong inversion region. The lowest energy level calculated from the full analytic model demonstrates an excellent accuracy, which is depicted in Fig. 5(b). Figure 6 shows that the full analytic model for the ballistic current also demonstrates the equivalent accuracy.

V. Circuit Simulation

An inverter circuit shown in Fig. 7(a) was simulated with the fully analytic model. We brought in the analytic expression of the ballistic current to HSPICE as a Verilog-A script. Figure 7(b) shows the output characteristic of the inverter circuit.

VI. Conclusion

An analytic and explicit compact model of the GAA-MOSFETs with rectangular cross section has been proposed. It demonstrates a high precision equivalent to the numerical compact model. In addition, we incorporated this fully analytic model to the circuit simulation as a Verilog-A script, and the circuit simulation of the inverter circuit was successfully demonstrated.

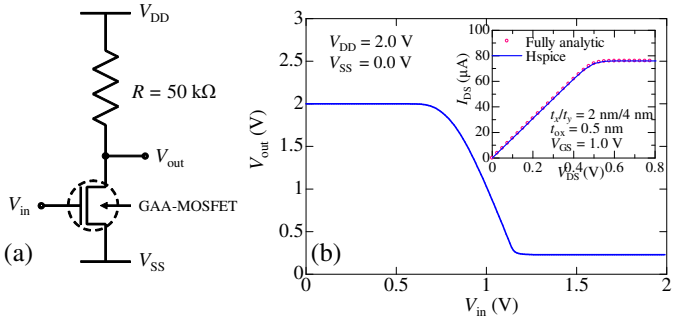

Fig. 7. (a) Schematic diagram of the inverter circuit. The fully analytic model of a GAA-MOSFET is introduced to HSPICE as a Verilog-A script. (b) The output voltage $V_{\rm out}$ of the inverter circuit simulated by a HSPICE simulator. The horizontal axis represents the input voltage $V_{\rm in}$. The inset shows that the ballistic current of the n-type GAA-MOSFET calculated from HSPICE demonstrates a good accuracy with the fully analytic model.

References

[1] J. Wang *et al.*: IEEE Trans. Electron Devices. **52** (2005) 1589.
[2] G. Mil'nikov *et al.*: J. Appl. Phys. **104** (2008) 044506.
[3] K. Natori.: IEEE Trans. Electron Devices. **55** (2008) 2877.
[4] A. Rahman *et al.*: IEEE Trans. Electron Devices. **50** (2003) 1853
[5] B. Iñiguez *et al.*: IEEE Trans. Electron Devices. **53** (2006) 2128.
[6] B. C. Paul *et al.*: IEEE Trans. Electron Devices. **54** (2007) 1637.
[7] T. Numata *et al.*: Jpn. J. Appl. Phys. **49** (2010) 04DN05.
[8] A. Aymerich-Humet *et al.*: J. Appl. Phys. **54** (1983) 2850.